I&EC research
Industrial & Engineering Chemistry Research

pubs.acs.org/IECR
Article

Phosphorus Dosing during Catalytic *n*-Butane Oxidation in a μ-Reactor: A Proof of Concept

Scott D. Anderson,* Martin Kutscherauer, Nicolas Nickel, Sebastian Böcklein, Gerhard Mestl, Gregor D. Wehinger, and Thomas Turek

Cite This: https://doi.org/10.1021/acs.iecr.3c02604

ABSTRACT: The selective oxidation of *n*-butane to maleic anhydride over vanadium−phosphorus oxide catalysts is subject to a dynamic change in the catalyst activity. This phenomenon is called phosphorus dynamics and plays a vital role in the prediction of catalytic reaction rates, but to date, no models measured under transport limitation free conditions have been published. This study presents the first investigation of the phosphorus dynamics over extended periods of time (multiple days on stream) under transport limitation free conditions in a μ-fixed-bed reactor. Initially, temperature variation experiments are conducted to investigate whether phosphorus dynamics takes place in a μ-reactor and to determine the onset of phosphorus loss. Then, a setup for dosing of liquid organophosphorous species on the scale of nL min^{-1} is proposed, and functionality is demonstrated via step test experiments. Results of the temperature variation showed that phosphorus loss occurs in the μ-reactor but starts at temperatures exceeding those of industrial scale reactors by 30−80 K. It was further observed that addition of steam to the feed increases the intensity of the phosphorus dynamics and lowers the onset temperature. Step test results demonstrated the functionality of the dosing setup if a suitable inert material is chosen and the metal surfaces downstream the dosing are treated according to a passivation procedure proposed in this study. The addition of steam appears to be required for appropriate distribution of the dosed organophosphorous species over the catalyst bed.

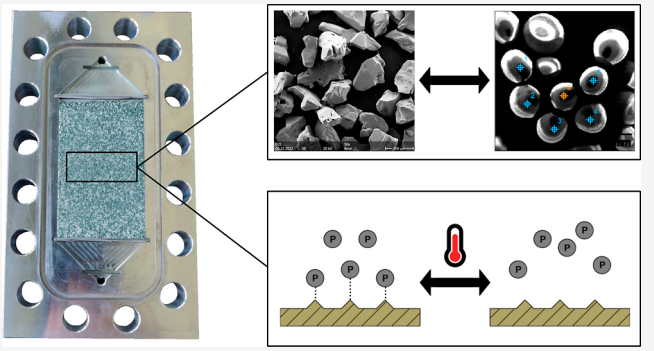

INTRODUCTION

Maleic anhydride (MA, IUPAC: Furan-2,5-dione) is an organic molecule that plays a vital role in the chemical industries. Its main uses are for unsaturated polyester resins, copolymers, lubricant additives, or as a precursor for other bulk chemicals.[1] The state-of-the-art process involves vanadium−phosphorus−oxide (VPO), a mixed metal oxide catalyst, that is used to selectively oxidize *n*-butane to MA. This process was developed by Chevron and Monsanto in the 1970s[2,3] and replaced the selective oxidation of benzene, which to date holds only minor relevance.[1]

The strongly exothermic ($-\Delta_R H = -1236$ kJ mol^{-14}) selective oxidation requires excellent heat-transfer properties of the catalytic reactor. At the same time, the low reactivity of *n*-butane warrants the reaction be carried out at high temperatures.[5,6] Therefore, industrial multitubular fixed-bed reactors consisting of several tens of thousands of tubes between 3.5 and 6.5 m in length and 21−25 mm in diameter are cooled via a molten salt bath at temperatures between 380 and 430 °C.[5,7] Despite the use of slender reactor tubes, a common issue with industrial MA reactors is the insufficient removal of heat, which leads to the formation of hot-spots in front of the catalyst bed. Maximum hot-spot temperatures of 50−70 K above the salt bath temperature have been reported in the literature.[6,7] Increased temperature leads to a higher catalytic activity, which favors the total oxidation toward CO_x. It is well known that consecutive MA combustion appears at *n*-butane conversions exceeding 70% .[8−10] A route of *n*-butane total combustion to CO_x via acrylic and acetic acid has also been reported.[8,9,11] The so-called phosphorus dynamics of the VPO catalyst exacerbate these issues: under reaction conditions, the catalyst experiences a loss of phosphorus, which also results in an increased catalytic activity with accompanying loss in selectivity. As the total oxidation of *n*-butane releases significantly more heat than the partial oxidation to MA, the total heat released increases, which can ultimately lead to thermal runaway. The loss of phosphorus is countered by adding organophosphorous species (1−3 ppm, usually trimethyl phosphate) to the reactor feed to replace the

Received: July 27, 2023
Revised: November 2, 2023
Accepted: November 3, 2023

lost phosphorus and maintain a constant activity of the catalyst.[5−7,10,12−16]

Improvement of the selectivity of the reaction by better reactor control, in particular regarding the temperature, holds enormous benefits in multiple regards. Besides increasing reactor safety by reducing the risk of thermal runaway, reducing the overoxidation of *n*-butane can increase the target product yield. In light of climate change, not only the production of MA but all selective oxidation reactions in general face additional pressure for reduction of CO_x emissions, which account for almost 80% of greenhouse gas emissions.[17,18] Due to the large scale of global MA production (3,000,000 t a^{-1} in 2018, individual plants with more than 100,000 t a^{-1}), even minor improvements have a significant impact.[1,19] In order to leverage this potential, a detailed understanding of all the processes (i.e., inter- and intraparticle mass and heat transport, catalytic reaction, and phosphorus dynamics) taking place in an industrial reactor is a fundamental requirement. This includes but is not limited to suitable models to describe the reaction and the phosphorus dynamics. While many reaction kinetics have been published,[10,11,19−26] only very few models include the phosphorus dynamics. Early on, Wellauer et al.[10] published a reactor model including a description of the dynamic catalyst activity. They hypothesized that the dominant deactivation phenomenon comprised sublimation of phosphorus on the catalyst and modeled this using an Arrhenius expression. Their findings suggested that reducing the hot-spot in the reactor results in increased MA yields. Diedenhoven et al.[13] published a conceptual model for the phosphorus dynamics based on reversible sorption processes. Later, Lesser et al.[19] published reaction kinetics coupled with a dynamic activity model for the phosphorus dynamics derived from pilot reactor measurements. Although the reactor performance could be described with remarkable precision over prolonged experiments under industrial conditions, both the reaction kinetics and the dynamic activity model include transport limitations due to the nature of the pilot reactor. Therefore, extensive reparameterization is necessary for applying them to any other reactor type or for use with a different reactor model. It becomes apparent that the modeling approaches rely heavily on simplifying assumptions rather than first principles, which is primarily grounded in the fact that the underlying physicochemical processes of the phosphorus dynamics have not been fully understood to date, as evidenced by the lack of topical literature.

Müller et al. published reaction kinetics that were measured under transport limitation free conditions using a specially designed slit reactor.[11,27,28] However, there is no model to describe the phosphorus dynamics available to date that was measured under limitation free conditions, as evidenced by the lack of literature. Since no evidence of phosphorus dynamics has been reported in previous studies using the slit reactor,[11,27−29] this study first addresses the question of whether phosphorus dynamics occur in this reactor through temperature variation experiments. Then, the experimental setup originally developed by Hofmann and Turek[29] and further improved by Müller et al.[27] is expanded by a setup for dosing organophosphorous compounds to lay the groundwork required for a limitation free phosphorus dynamics model. Step tests with phosphorus dosing are performed to demonstrate the operability of the dosing setup, and first observations concerning the phosphorus dynamics made during these experiments are reported.

METHODS

Experiments were conducted in a slit fixed-bed reactor (hereafter referred to as μ-reactor) originally developed by Hofmann et al.[29] and further improved by Müller et al.[27] as shown in Figure 1. Only a brief summary of the experimental

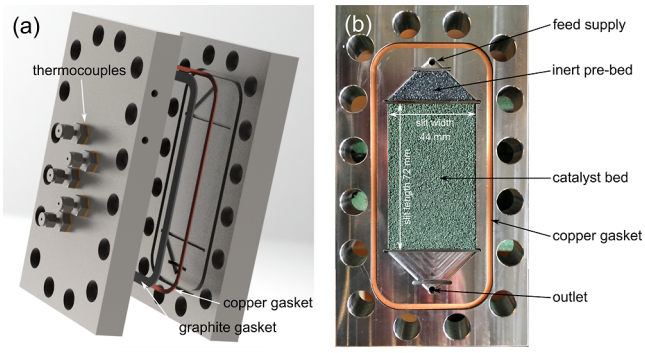

Figure 1. (a) CAD model of the μ-reactor with gaskets and (b) μ-reactor backing plate with catalyst bed and inert pre-bed.[27] 2019 Müller et al. Published by WILEY-VCH Verlag GmbH & Co. KGaA, Weinheim.

setup is given here; the authors refer the reader to the Supporting Information (chapters S1−S3) and the original publications by Hofmann et al.[29] and Müller et al.[27] for a more detailed description.

The μ-reactor setup involves two stainless steel plates with a milled insert that holds the catalytic μ-fixed-bed. Both plates are mounted together via 16 M12 × 50 bolts and sealed with copper and graphite gaskets. Industrial VPO catalyst (Clariant SynDane) was milled and sieved, and inert materials are added when necessary to dilute the fixed-bed. Further information regarding the milling and preparation of the μ catalyst can be found in chapter S4 in the Supporting Information. Either silicon carbide (SiC, Alfa Aesar 46 Grit) or steatite (Mühlmeier GmbH & Co. KG, Bernau) were used as inert materials in the experiments. The reactor is submerged in a molten salt bath (45/55 wt % $NaNO_3/KNO_3$) for precise temperature control (380−460 °C).

To investigate the phosphorus dynamics, the pre-existing plant was expanded for phosphorus dosing setup involving a push/pull syringe pump (Fink Chem + Tec LSP01−1C). TMP (Merck ≥98%) is used as organophosphorous compound, and the industrially relevant concentration ranges (1 ppm and 5 ppm[6,30]) result in flow rates between 1 nL min^{-1} and 1 μL h^{-1}.

RESULTS

Before attempting phosphorus dosing, it was tested whether phosphorus loss occurs in a μ-reactor the same way it is found in larger scale industrial and pilot reactors. Then, step test experiments were carried out to test whether the previously proposed phosphorus dosing setup was operational.

Forcing Phosphorus Loss in the Reactor. In previous publications,[11,27,28] the phosphorus dynamics could not be observed in the μ-reactor. Under moderate reaction conditions (temperature: 430 °C and gas hourly space velocity (GHSV): 4800 m^3 m^{-3} h^{-1}) even after up to 80 days on stream, *n*-butane conversion and MA selectivity remained constant, indicating

https://doi.org/10.1021/acs.iecr.3c02604
Ind. Eng. Chem. Res. XXXX, XXX, XXX−XXX

Table 1. Parameters for the Temperature Variation Experiments Determined from a 1D−1D Heterogeneous Model and Steady-State Values[a] for Conversion and Selectivities as Well as the Error of the Oxygen Balance

exp	point	T_{SBT} °C	GHSV $m^3\ m^{-3}\ h^{-1}$	$\overline{X}_{C_4H_{10}}$%	$\overline{S}_{MA}$%	$\overline{S}_{CO}$%	$\overline{S}_{CO_2}$%	$\overline{\epsilon}_{O_2}$%
1	1	430	2550	65.1	69.5	18.4	12.0	0.38
1	2	440	3200	65.7	68.5	19.4	12.1	0.63
1	3	450	3950	65.0	67.2	20.5	12.4	1.25
1	4	460	4800	n.a.	n.a.	n.a.	n.a.	n.a.
1	5	430	2550	73.3	60.7	24.5	14.7	−0.25
2	1	430	2550	59.5	73.5	14.3	12.2	−5.12
2	2	440	3200	62.4	73.1	15.3	11.6	−5.69
2	3	450	3950	n.a.	n.a.	n.a.	n.a.	n.a.
2	4	460	4800	n.a.	n.a.	n.a.	n.a.	n.a.
2	5	430	2550	74.6	66.2	18.4	15.5	−6.05

[a]n.a. where no steady state was reached.

that no phosphorus loss had taken place. This observation is in stark contrast to Lesser,[7,19] who reported significant phosphorus loss in a pilot reactor at much lower inlet temperatures (400 °C) but at similar *n*-butane conversion.

In order to determine whether the phosphorus dynamics was taking place in the μ-reactor, a systematic variation of reactor operating temperature was carried out. As the available literature clearly reports a strong effect of water on the phosphorus dynamics and the composition of the catalyst surface,[7,12,19,30−35] this temperature variation was repeated under both dry feed conditions and with 2 mol % steam added to the feed. Due to the broad range of investigated temperatures, measures had to be taken to ensure that the *n*-butane conversion stays within the range of industrial conditions and to avoid total conversion at elevated temperatures: the catalyst bed was diluted with inert SiC particles, the contact time was varied via the GHSV, and the corresponding operating points are given in Table 1. A 1D−1D-heterogeneous reactor model, originally published by Müller et al.,[11] was used to determine the required GHSV values for each temperature in order to maintain an *n*-butane conversion within the industrially relevant range (65−85%).

For the first experiment under dry feed conditions, the μ-reactor was loaded with 5.52 g of inert SiC and 2.18 g of catalyst. The pre-bed consisted of 0.95 g of inert SiC. After an initial startup phase, the salt bath temperature T_{SBT} was increased in increments of 10 K. The feed stream comprised a mixture containing 1.5 mol % *n*-butane and 20.685 mol % O_2 and the remainder composed of N_2. For each operating point, the temperature was increased once a new steady state of *n*-butane conversion $X_{C_4H_{10}}$ and MA selectivity S_{MA} was reached, indicating that no phosphorus loss was taking place. Once the phosphorus loss had begun and was maintained for a certain time, T_{SBT} was reduced back to 430 °C to allow for comparison to the initial operating point. A total overview of the tested conditions is given in Table 1, where N_2 made up the remainder of the feed composition.

Figure 2 shows the *n*-butane conversion $X_{C_4H_{10}}$ and the MA selectivity S_{MA} as well as the salt bath temperature T_{SBT} during the first experiment with dry feed. During the first 14 days on stream, the catalyst undergoes an equilibration stage, characterized by a decrease in *n*-butane conversion $X_{C_4H_{10}}$ and an increase in MA selectivity S_{MA}, where both conversion and selectivity approach a steady state. Once a steady state had been reached, the temperature variation was started. It can be seen that the *n*-butane conversion remains steady for

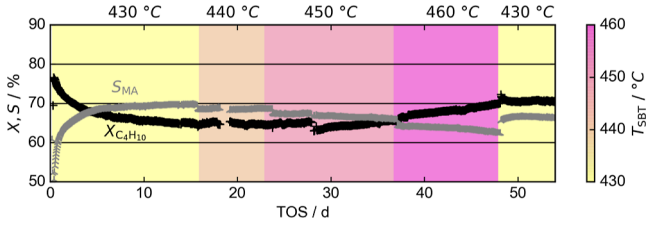

Figure 2. Trajectories of *n*-butane conversion $X_{C_4H_{10}}$ and MA selectivity S_{MA} over the course of temperature variation with dry feed stream to determine the onset temperature of phosphorus loss in the μ-reactor.

temperatures T_{SBT} < 460 °C at ca. 65%, thereby indicating no phosphorus loss.

At 27.8 days on stream and T_{SBT} = 450 °C, a sudden drop in *n*-butane conversion appears. This is due to a power shortage, where the experimental plant shuts down and the catalyst bed was perfused with N_2. After subsequent startup of the reaction, the catalyst gradually increases activity again, which results in the observed drop. Interestingly, the MA selectivity drops with increasing temperature but remains steady at each temperature. After increasing T_{SBT} to 460 °C at 39 days on stream, the *n*-butane conversion begins to increase gradually accompanied by a decrease in MA selectivity, which is indicative of phosphorus loss on the catalyst, where the catalyst becomes more active and less selective. Within 10 days on stream at 460 °C, the *n*-butane conversion increases by 3.2%, and the MA selectivity drops by 1.8%. After reducing the salt bath temperature T_{SBT} back to 430 °C, both conversion and selectivity become stable again at ca. 70 and 67%, respectively. Comparison with the initial values at 430 °C (operating point 1) shows an increase of 5% in *n*-butane conversion and a decrease of 3% in MA selectivity (compare Table 1). This deviation further indicates that the catalyst has undergone phosphorus loss, resulting in a permanent increase in catalytic activity.

Figure 3 shows the second temperature variation experiment, which was conducted with the addition of water to the feed stream. The μ-fixed-bed was composed of 5.53 g of inert SiC and 2.19 g of catalyst. The pre-bed consisted of 0.96 g of inert SiC. A mixture of 1.5 mol % *n*-butane, 20.265 mol % O_2, and 2 mol % H_2O was fed to the reactor. The remainder of the feed stream consisted of N_2. Again, after 10 days on stream for equilibration of the catalyst, a steady state characterized by an *n*-butane conversion of $X_{C_4H_{10}}$=60% and a MA selectivity of

https://doi.org/10.1021/acs.iecr.3c02604
Ind. Eng. Chem. Res. XXXX, XXX, XXX−XXX

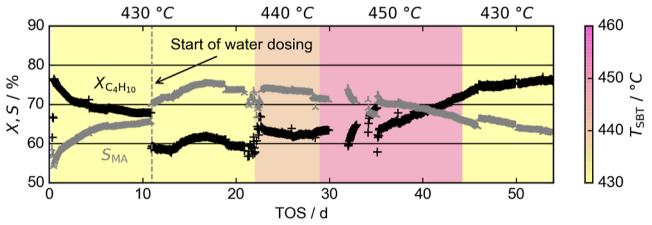

Figure 3. Trajectories of *n*-butane conversion $X_{C_4H_{10}}$ and MA selectivity S_{MA} over the course of temperature variation with 2% steam added to the feed stream to determine the onset temperature of phosphorus loss in the μ-reactor.

S_{MA} = 74% is reached. For the subsequent higher temperature of 440 °C, a new steady state ($X_{C_4H_{10}}$=63%, S_{MA} = 73%) is obtained within 1 day on stream after increasing the temperature, as well. At a salt bath temperature of 450 °C, the phosphorus loss begins with the characteristic increase in *n*-butane conversion and decrease in MA selectivity. Within 16 days on stream at 450 °C, the *n*-butane conversion increases by 10.5% and the MA selectivity drops by 7.3%. As the phosphorus loss already began at 450 °C, testing at 460 °C was skipped. After returning T_{SBT} to 430 °C, the conversion becomes constant at ca. 75%, while the selectivity is at 67%. Comparing this to the values around 20 days on stream, a permanent increase in conversion of 15% was found alongside a decrease in selectivity of 7%, again indicating permanent phosphorus loss of the catalyst.

The presented data are of a global nature and do not provide any information concerning the events transpiring at the catalyst surface. To ensure that the observed changes in conversion and selectivity are indeed caused by the phosphorus dynamics and are not a product of unrelated ageing phenomena, postreaction samples of the catalysts from both experiments were procured and characterized. No samples could be drawn directly prior to the invoked activity increase, as this requires disassembly of the μ-reactor, which subsequently terminates the experiment. Instead, a sample of fresh, nonequilibrated catalyst was characterized for comparison. Physisorption measurements and Hg-porosimetry were conducted to determine the specific surface area and porosity (detailed description of measurements given in the Supporting Information). The measured data are listed in Table 2.

Table 2. Specific Surface Areas and Porosity for the Catalyst Samples

sample	specific surface area $m^2\ g^{-1}$	porosity %
fresh	23.6	38.50
spent (dry feed)	18.9	40.60
spent (wet feed)	21.3	39.87

While the fresh catalyst has a specific surface area of 23.6 $m^2\ g^{-1}$, the spent catalyst samples show slightly reduced surface areas (18.9 and 21.3 $m^2\ g^{-1}$) in comparison. Ihli et al.[36] reported specific surface areas of 6 $m^2\ g^{-1}$ (hot-spot) and 11 $m^2\ g^{-1}$ (inlet) for the same type of commercial catalyst extracted from an industrial reactor after 4.5 years on stream. They also reported a surface area of 20 $m^2\ g^{-1}$ for a pristine catalyst particle. In the present study, the catalyst displayed specific surface areas that more closely match those reported by Ihli et al. for the pristine catalyst rather than the reduced surface areas of the aged catalyst. Moreover, it is noteworthy that the extended time frame leading to the reported aging effects exceeds the duration of the experiments presented in this work, suggesting that ageing effects are unlikely contributors to the reported activity increases. The porosity is similar for the fresh catalyst and both postreaction samples; all the three measurements lie in the vicinity of 40% (38.5, 40.5, and 39.87%, respectively).

The characteristic reduction of *n*-butane conversion with parallel gain in MA selectivity observed in Figures 2 and 3 has been reported in other experimental studies as well.[11,19,27,28,30,37] A recent review[6] attributes the initially high activity to vanadyl-pyrophosphate (VPP) defect structures which make lattice oxygen more available. Granados et al.[38] reported higher oxygen availability in fresh VPO catalyst, whereas the higher selectivity of the activated catalyst was explained by desorption of reaction products at lower temperatures. These defects however heal over time such that the activity is reduced during the first few days on stream.[39] Gai et al.[40] demonstrated that within the first 100−300 h, VPO catalysts undergo microstructural changes on the surface under *n*-butane oxidation conditions. Considering the mentioned studies, the observed behavior of the catalyst during equilibration is in excellent agreement with the literature, indicating that the same processes are taking place as in much larger scale reactors.

It was further observed that, despite the *n*-butane conversion remaining constant between temperature increases, the MA selectivity decreased further with each temperature increment. While a decrease in contact time (increased GHSV) is sufficient to keep the conversion constant, this seems not to be the case for the selectivity. Buchanan and Sundaresan[26] as well as Bej and Rao[41] reported higher activation energies for the unselective oxidation reactions compared to the selective oxidation, thereby indicating that elevated temperatures are detrimental for MA selectivity. Therefore, the reduction of contact time will help maintain the conversion even at higher temperatures, but the selectivity is still affected, thus resulting in the observed stepwise reduction of S_{MA}.

Interestingly, the previous results demonstrate that phosphorus loss begins earlier and is more intense when steam is added to the feed. During the first temperature variation experiment, the *n*-butane conversion increases with a rate of 0.32%/DOS, and the MA selectivity drops with a rate of −0.18%/DOS. When steam is added to the feed, the *n*-butane conversion change rate almost doubles to 0.66%/DOS, whereas the MA selectivity change rate increases by a factor of almost 2.6 to −0.46%/DOS. In the patent literature, it was observed that steam exhibited a distributing effect on phosphorus along the fixed-bed.[12] It was also observed that addition of steam to a phosphorus rich catalyst reduces the surface concentration of phosphorus and increases the catalyst activity.[12,30−32,42,43] Lesser et al.[7] reported a strong influence of feed steam content on the phosphorus dynamics in a pilot reactor. Two explanations were proposed: either there is competitive adsorption of water and phosphorus or the dynamic surface changes on the catalyst caused by the steam influence the absorption capacity of the catalyst for phosphorus.

Multiple other authors have reported that addition of steam to the feed increases the P/V ratio on the catalyst surface by converting V−O−P groups to terminal hydroxyl groups on both phosphorus and vanadium.[31−35] Arnold and Sundaresan[31] suggested that the presence of steam leads to a decrease

https://doi.org/10.1021/acs.iecr.3c02604
Ind. Eng. Chem. Res. XXXX, XXX, XXX−XXX

in coordinatively unsaturated vanadium species. These vanadium species exhibit a high affinity toward the catalyst surface and thereby displace phosphate groups toward the catalyst bulk. It is conceivable that a decrease in coordinatively unsaturated vanadium species would allow phosphate groups to reach the catalyst surface more easily, thereby reducing the energy barrier for phosphorus loss on the catalyst surface. While in agreement with the experimental observations of Lesser et al.,[7] who observed that water reduces the phosphorus concentration on the catalyst surface, as well as those observations reported in this work, it has to be emphasized that the previous conceptions are purely hypothetical and should not be taken as a fact. Extensive surface characterization is required for further investigation of this hypothesis.

On the basis of the presented experiments, it becomes apparent that phosphorus loss does indeed take place in the μ-reactor. In good agreement with the literature on the catalyst performance, both under industrial and laboratory conditions as well as analytical studies on the surface composition, it was observed that addition of steam to the feed leads to phosphorus loss onset at lower temperatures. Owed to the coarse steps of the temperature variation experiments, a clear temperature for the phosphorus loss onset under the investigated conditions cannot be discriminated. Rather, it can only be stated that phosphorus loss began at $T_{SBT} > 450$ and >440 °C for dry and wet conditions, respectively.

It was also found that the required temperature for phosphorus loss drastically exceeded those reported in studies using larger reactor types: Lesser et al.[7,19] reported phosphorus loss at an inlet temperature of 400 °C. The disparity between the pilot reactor used by Lesser et al.[7,19] and the μ-reactor is likely rooted in the size of the catalyst particles used. While the pilot reactor is essentially a single tube of an industrial reactor and hence uses industrial catalyst particles ($d_{p,outer} \approx 4.7$ mm, $d_{p,inner} \approx 1.7$ mm, and $h \approx 4.7$ mm[36]), the μ-reactor is filled with milled particles in the size range of 430 μm < d_p < 630 μm. The temperatures measured in the pilot reactor via an axial thermocouple may therefore accurately describe the gas-phase temperature but are likely not representative of the temperature the individual particles experience; rather, the temperatures on the particles will be much higher. Computational fluid dynamics simulation studies have even shown that particles can experience temperature differences of up to 40 K on their surface.[44] In contrast, Müller et al.[27] calculated a catalyst effectiveness of usually $\eta_{cat} > 95\%$ for the milled particles, thereby proving the absence of transport limitations, which results in identical salt bath, gas phase, and solid temperature in the μ-reactor. This explains why the μ-reactor does not show any phosphorus loss at the temperatures reported by Lesser et al.[7,19] but require much higher temperatures.

The strong discrepancy in phosphorus loss onset temperature between the pilot and the μ-reactor also highlights once again the importance of transport limitation free measurements for kinetic model parameterization. The elevated temperatures in the catalyst particles are not captured by the temperature measurements; therefore, the reaction rates are attributed to lower temperatures than actually present, which ultimately results in erroneous kinetic parameters in the model. Essentially, the reaction kinetic model will contain transport limitations in its parameters. In practice, this results in need for extensive reparameterization of the model when applied to other reactor types or used with different models (e.g., 1D−1D vs 2D−1D), which is often not feasible. Ideally, the kinetic model should not contain any transport limitations and be universally applicable to any reactor type in combination with a suitable reactor model that accounts for transport phenomena.

Step Test Experiments. A step test experiment was conducted to prove the functionality of phosphorus dosing. In order to avoid damage to the catalyst by excessive addition of phosphorus, the experiment was conducted at a temperature where phosphorus loss was observed in previous experiments. This way, a dampening effect should be visible either through decreasing the catalyst activity or through stopping or slowing the increase of the catalyst activity. Because of the elevated temperatures, a diluted catalyst bed consisting of 2.15 g of VPO catalyst and 5.71 g of inert SiC was used, together with a pre-bed of 1.01 g of SiC. Initially, the reactor was operated at a temperature of 430 °C and a GHSV of 2550 $m^3\ m^{-3}\ h^{-1}$ and fed with a mixture of 1.5 mol % *n*-butane and 20.685 mol % O_2 where the remainder was made up of N_2. Under these conditions, the catalyst was activated for approximately 15 days on stream until a steady state of conversion and selectivity was reached. Thereupon, an initial activity increase was evoked by increasing the salt bath temperature to 450 °C and adding steam to the feed (2 mol %), such that the catalyst activity would not decrease to conversions at subindustrial levels as a result of the phosphorus dosing. To maintain constant conversion, the GHSV was raised to 3950 $m^3\ m^{-3}\ h^{-1}$. After a sufficient increase in *n*-butane conversion, the phosphorus dosing was started in the hope of either reaching a new steady state of conversion and selectivity or even reversing the catalyst activity increase.

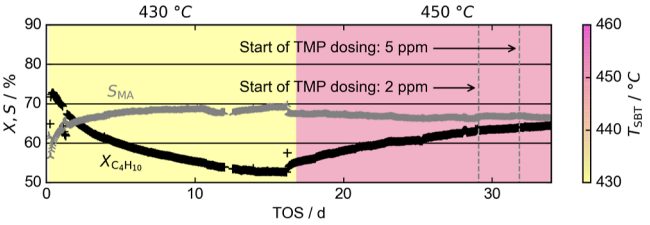

Figure 4. Initial step test experiments were conducted to determine whether the syringe pump setup was capable of dosing phosphorus to the μ-reactor.

Figure 4 shows the trajectories of *n*-butane conversion $X_{C_4H_{10}}$ and MA selectivity S_{MA} over the time on stream. Initially after startup, the *n*-butane conversion shows the highest levels during the experiment, at 72.9%, while the MA selectivity starts at around 55.0%. Within the following days on stream, the conversion gradually reduces, while the selectivity increases until both stabilize at 15 days on stream around 52.8 and 68.9%, respectively. The conversion is significantly lower than in the previous experiments (compare Figures 2 and 3). This is likely attributable to a calibration issue with the butane MFC. While the absolute values from this experiment can therefore not be used for direct comparison, the consistent nature of the calibration error still allows assessment of the relative changes in conversion and selectivity. Hence, the data can be utilized to determine whether damping via phosphorus dosing occurs, regardless. Upon increasing the salt bath temperature at 16 days on stream from 430 to 460 °C, the *n*-butane conversion begins to rise, while the MA selectivity decreases. At 29.5 days

https://doi.org/10.1021/acs.iecr.3c02604
Ind. Eng. Chem. Res. XXXX, XXX, XXX−XXX

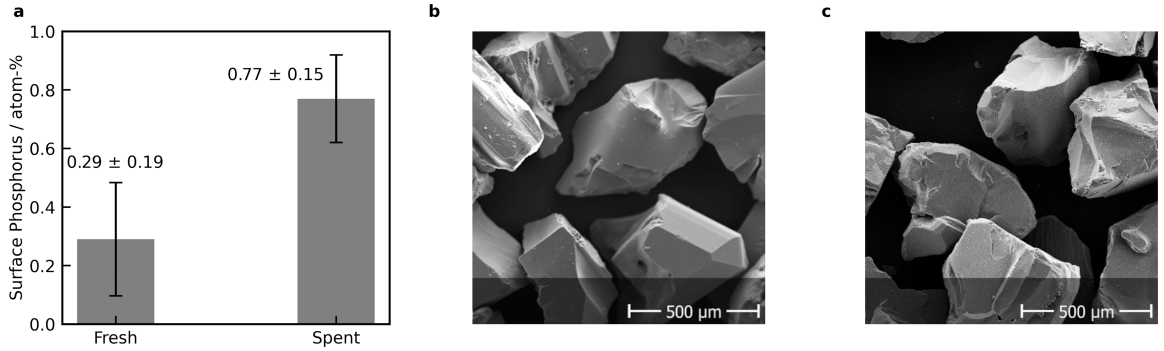

Figure 5. EDX measurements show (a) how SiC samples taken from the inert pre-bed after the phosphorus dosing step test have higher phosphorus content on the surface than fresh SiC samples. SEM images from the spent (b) and fresh (c) samples show no obvious differences.

on stream, TMP dosing is started with a feed concentration of 2.3 ppm, while at a temperature where phosphorus loss was previously observed. Within the following 2 days on stream, no significant reduction in activity increase is visible, the *n*-butane conversion increases a further 0.5%. Due to underlying data scatter, no clear trend in MA selectivity during this time can be identified. Therefore, at 31.5 days on stream, the amount of TMP dosed was increased to a feed concentration of 5 ppm. However, within the following 2 days on stream, the activity increase still did not show signs of damping through the phosphorus dosing. The *n*-butane conversion increased a further 0.45% to a total of 64.5%, while the MA selectivity fell to 66.2%. It was therefore concluded that no phosphorus had reached the catalyst bed, and the experiment was terminated.

A caveat to the aforementioned conclusion is that there were two superimposed effects acting during phosphorus dosing. While the addition of TMP to the feed should reduce the catalyst activity, the temperature was still sufficiently high to cause an activity increase. One can easily imagine that the amount of dosed phosphorus was simply insufficient to counteract the activity increase caused by the elevated salt bath temperature. However, in pilot- and industrial scale reactors, the range of dosed phosphorus ranges from 1 to 3 ppm at most.[6] While it might be suspected that the μ-reactor requires more phosphorus than an industrial reactor, based on the fact that the entire catalyst bed experiences the elevated temperatures rather than just the catalyst particles in the hot-spot region, even the addition of supraindustrial levels (5 ppm) did not affect the activity increase. This exceeds the common phosphorus concentration in industrial reactors by 500%, which the authors were confident would dampen the catalyst activity significantly. As this was not observed, it must be concluded that either only a fraction of the phosphorus or no phosphorus at all had reached the catalyst bed.

A root cause analysis was conducted and excluded the pump, valve, and piping to the feed lines as the problems. Separate tests, measuring the amount of liquid dosed over a defined time interval, concluded that the pump setup worked as intended (measurements were taken at the point of entry to the main feed line). It was therefore suspected that the problem must lie in the feed lines between the pump and the reactor. It is unknown which phosphorus-containing species forms in the gas phase, as TMP thermally decomposes when heated.[45] A literature research revealed several studies on the corrosion behavior of stainless steel in the presence of phosphoric acid, which have reported the formation of phosphorus-containing protective layers.[46−48] Based on these findings, it was assumed that the dosed phosphorus adsorbs on the surface of the stainless steel piping and forms similar structures. To mitigate the suspected phosphorus adsorption on the steel piping, a passivation protocol was devised and is described in chapter S3 in the Supporting Information. As the reactor plates were passivated as well and the catalyst material itself is unlikely to be a problem, SiC as the inert dilutant was suspected as a possible cause for the observed problems as well. Energy-dispersive X-ray spectroscopy (EDX) measurements of selected SiC samples from the inert pre-bed as well as from fresh dilutant were carried out with a scanning electron microscope (SEM, Zeiss DMS 982 Gemini). Figure 5 shows the qualitative results comparing the fresh and spent samples as well as two SEM images. Comparing Figure 5b,c reveals that the SiC particles have undergone no optical change during the experiment. It becomes readily apparent how the sample from the inert pre-bed shows a significantly more intense phosphorus signal on the surface than the fresh sample, even when considering the standard deviation of the measurements. It was suspected that phosphorus adsorbs to SiO_2 present at the surface of the dilutant material. Therefore, for further experiments, it was decided to use steatite instead. Steatite is a magnesium−silica ceramic material that is sintered at high temperatures, which should remove any surface hydroxyl groups from the material and mitigate the formation of the aforementioned phosphorus species on the surface.

After all plant parts downstream of the phosphorus dosing were passivated according to the previously described procedure, the step test experiments were repeated. Unlike in the previous experiments, the step test was conducted at lower temperatures (T_{SBT} =430 °C), and therefore, an undiluted bed of catalyst (5.55 g of VPO, no inert material or pre-bed) was used. The reactor was fed with a mixture of 1.5 mol % *n*-butane, 20.685 mol % O_2, and remainder N_2 at a GHSV of 4800 $m^3\ m^{-3}\ h^{-1}$. Thereby, any effects of dilutant material on the functionality of phosphorus dosing could be excluded, and the passivation of the metal surfaces could be examined. Additionally, the superimposition of phosphorus loss and phosphorus dosing was avoided. As in the previous experiment, once a steady state was reached, the phosphorus dosing was started until a new steady state was reached. Then, the phosphorus dosing was stopped. This was repeated for a second time using a higher phosphorus content.

Figure 6 shows the trajectories of *n*-butane conversion, MA, CO, and CO_2 selectivity over the course of this experiment. The development of the axial temperature profile, as measured by the five axial thermocouples, is shown in Figure 7. A

https://doi.org/10.1021/acs.iecr.3c02604
Ind. Eng. Chem. Res. XXXX, XXX, XXX−XXX

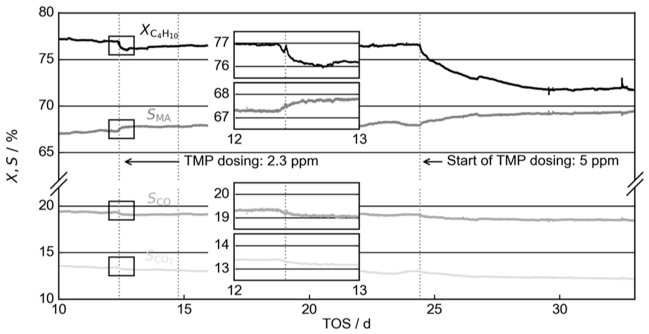

Figure 6. Phosphorus addition during step test experiments at lower temperatures resulted in reduced catalytic activity.

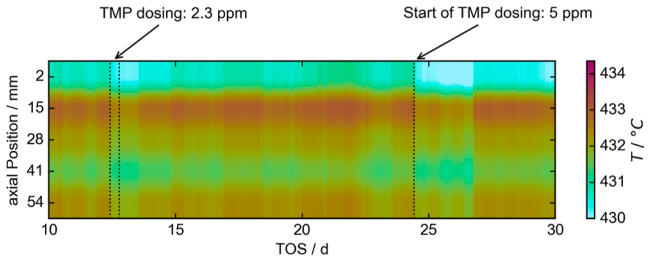

Figure 7. Axial temperature profile taken from five thermocouples over the step test experiments.

summary of the described steady states is given in Table 3. After equilibration under dry feed conditions, the reactor reached a steady state at approximately 10.75 days on stream. This steady state is characterized by an *n*-butane conversion of 76.9%, MA selectivity of 67.3%, and CO and CO_2 selectivities of 19.3 and 13.4%, respectively. From the temperature profile, it can be seen that the catalyst bed shows slightly elevated temperatures at the second, third, and fifth thermocouple (15 mm, 28 mm, and 54 mm, respectively). After the first steady state was reached, phosphorus dosing was commenced at a time of 12.4 days on stream with a phosphorus concentration of x_{TMP} = 2.3 ppm. Within approximately 0.25 days on stream, the catalyst reached a new steady state, such that the phosphorus dosing was stopped at 12.78 days on stream. During this time, the *n*-butane conversion had decreased by 0.7%, MA selectivity increased by 0.5%, while the selectivity of CO and CO_2 both decreased by 0.25%. Immediately after phosphorus dosing began, the reactor temperatures decreased by ΔT < 1 K. After the phosphorus dosing was stopped at 12.78 days on stream, the catalyst was left in a dry feed until 24.4 days on stream. During this time, the catalyst activity did not return to its state prior to phosphorus dosing: the *n*-butane conversion increased slightly to 76.6%, which lies between the state prior to and post TMP dosing. The MA selectivity remained at 67.9%, the CO and CO_2 selectivity at 19.1 and 13%, respectively. At around 15 days on stream, the reactor temperatures had increased slightly to levels prior to phosphorus dosing again. At 24.4 days on stream, a second step test was conducted with a TMP feed concentration of 5 ppm. It took until 29.5 days on stream to reach a new steady state, which was characterized by a drop in *n*-butane conversion of 4.8%, an increase of 1.3% in MA selectivity and a decrease of 0.6 and 0.7% in CO and CO_2 selectivity, respectively. Again, the reactor temperatures immediately decreased as a response to the phosphorus dosing. At approximately 27 days on stream, the reactor temperatures had increased slightly again. The first axial thermocouple, at 2 mm, measured a slightly lower temperature than prior to dosing of 5 ppm TMP (430.7 vs 430.3 °C), despite the remaining temperatures increasing. The second thermocouple, at 15 mm, even measured a higher temperature than before.

The described behavior under phosphorus dosing is in good agreement with phosphorus dosing studies in pilot reactors.[7,19,30] Once the phosphorus dosing is stopped, however, the catalyst activity does not return to the state prior to dosing, which is in disagreement with the observations in the literature, where the adsorption of phosphorus was described as a fully reversible process.[7,19,30] The minor increase in *n*-butane conversion between 13 and 24.4 days on stream cannot be attributed to a specific effect; likely it is due to data scatter.

A further step test experiment was carried out to examine the inert dilutant material. A catalyst bed consisting of 2.501 g of VPO catalyst and 4.501 g of steatite with a steatite pre-bed (0.94 g) was tested. The reactor was operated at 430 °C with a feed stream of 1.5 mol % *n*-butane, 20.685 mol % O_2, and remainder N_2 at a GHSV of 2550 $m^3\ m^{-3}\ h^{-1}$. In order to avoid superimposition of phosphorus loss and phosphorus dosing, it was carried out at 430 °C, where no phosphorus loss occurs. For conversion within industrially relevant conditions, the contact time was increased (GHSV 2550 $m^3\ m^{-3}\ h^{-1}$) to counteract the effect of diluting the fixed-bed. The results of the third step of the test experiment are shown in Figure 8.

Analogous to previous experiments, the catalyst was first brought into a steady state following the equilibration of the catalyst. A *n*-butane conversion of 65.9% and a MA selectivity of 66.1% ensued. At 21.3 days on stream, the phosphorus dosing was commenced with a TMP feed concentration of 2 ppm and kept up until 23.4 days on stream. During this time, the *n*-butane conversion dropped by 1.5% and MA selectivity increased by 0.3%. No clear trend in CO and CO_2 selectivity can be identified due to data scatter. A reduction in conversion alongside increase MA selectivity strongly suggests a decrease in the selectivity to both CO and CO_2 by decreased overoxidation though. In the following days on stream (not shown in Figure 8), the catalyst did not return to its original activity as prior to phosphorus dosing.

The qualitative behavior observed in this third step test is in line with previous results. Addition of phosphorus to the feed reduces the catalytic activity, decreasing *n*-butane conversion and increasing MA selectivity, thereby proving the functionality of steatite as an inert dilutant for phosphorus dosing

Table 3. Steady Operating States during the Phosphorus Dosing Step Test Experiments

time DOS	<keep-togeher>$X_{C_4H_{10}}$ %</keep-togeher>	SMA %	SCO %	<keep-togeher>S_{CO_2} %</keep-togeher>	comment
10.75	76.9	67.3	19.3	13.4	steady state after equilibration
12.75	76.2	67.8	19.05	13.15	steady state after 2.3 ppm TMP dosing
24	76.6	67.9	19.1	13	steady state before 5 ppm TMP dosing
29.5	71.8	69.2	18.5	12.3	steady state after 5 ppm TMP dosing

https://doi.org/10.1021/acs.iecr.3c02604
Ind. Eng. Chem. Res. XXXX, XXX, XXX−XXX

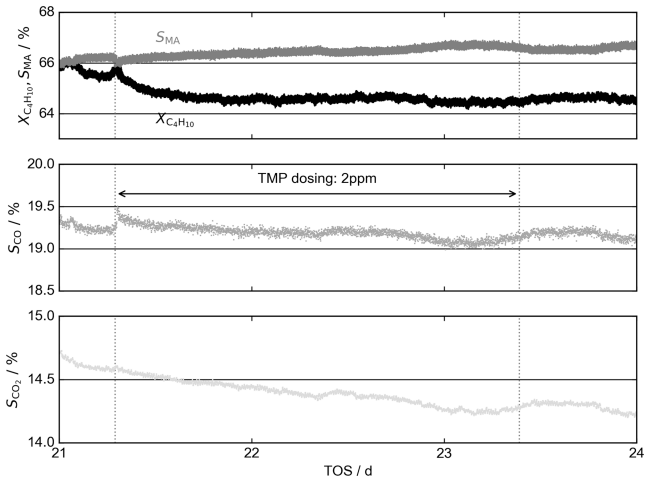

Figure 8. Dosing phosphorus to the feed of a fixed-bed of VPO catalyst diluted with steatite yields the same behavior as previously observed. *n*-Butane conversion and CO_x selectivity are retarded, whereas the MA selectivity increases.

experiments and confirming the previously postulated hypothesis.

The results observed in the step tests suggest that the phosphorus does not simply enter a sorption equilibrium where it covers active sites, such as proposed by Diedenhoven et al.[13] and Lesser et al.[19] If this were the case, after sufficiently long times, all phosphorus would have desorbed, returning the catalyst to its initial state; however, it was clearly observed that this is not the case. Instead, the phosphorus must be somehow incorporated into the catalyst structure following initial adsorption on the surface. Cavani et al.[49] found that even small amounts of phosphorus could influence the surface morphology of the catalyst via its P/V-ratio. On this basis, it could be speculated that the dosed phosphorus is incorporated into the VPO structure and changes the catalyst surface as well. The reversibility observed in the pilot reactor studies might be rooted in the fact that hot-spot and intraparticle temperatures may well exceed the measured gas phase temperatures, and therefore, the catalyst is undergoing superimposed phosphorus loss at the same time. This would translate to a higher activation energy for the desorption of the newly incorporated phosphorus species, which is reached only through the elevated temperatures in the pilot reactor. In contrast, due to the transport limitation free nature of the μ-reactor, the μ catalyst is not undergoing phosphorus loss, as these elevated temperatures are not reached.

When comparing the time required to reach a new steady state (in the second step test experiment, compare Figure 6), it becomes obvious that with a TMP concentration of 5 ppm, it takes significantly longer than with 2.3 ppm. Several studies and patents have reported that steam exhibits a distributing effect on phosphorus.[12,30,42,43] As all of the phosphorus dosing step test experiments presented in this study were conducted in a dry feed stream, it is conceivable that the absence of a distributing agent leads to an inhomogeneous phosphorus content within the fixed-bed. The temperature profile in Figure 7 shows how after dosing 5 ppm TMP, the temperature permanently decreases at the first thermocouple but increases after a few days on stream at the second thermocouple. This indicates deactivation of the catalyst bed around the first thermocouple, which results in more reactant-rich gas reaching the catalyst bed around the second thermocouple. This then results in higher turnover, releasing more heat, and increasing the temperature. It appears as though with 5 ppm TMP dosing the phosphorus accumulates around the first few layers of the catalyst bed due to a lack of steam to distribute the phosphorus along the entire bed evenly, causing the elevated temperatures further downstream of the bed.

CONCLUSIONS

A transport limitation free μ-reactor was expanded by a setup to dose and evaporate liquid organophosphorous compounds on a scale of a few nL min^{-1}. This now allows for the investigation of the phosphorus dynamics of the VPO catalysts.

Initially, it was shown that phosphorus loss does takes place in the μ-reactor, despite what has been shown in previous studies;[11,27,28] however, temperatures significantly higher (30−80 K) than in industrial reactors are required to evoke phosphorus loss. In further phosphorus dosing step tests, it was found that the dosed organophosphorus compounds adsorb on metal surfaces and on certain inert materials used for diluting the catalyst bed. A passivation procedure was applied to mitigate adsorption on surfaces, and a ceramic inert material sintered at high temperatures was used as an alternate dilutant.

Based on the results presented in this study, the following rules-of-thumb for phosphorus dosing experiments are proposed:

1. All surfaces downstream the phosphorus dosing should be subjected to a passivation procedure.
2. The choice of the inert material should account for binding of phosphorus on the catalyst. The preferable choice for inert materials is ceramics sintered at high temperatures to remove surface oxygen.

It remains possible that there may not be a need for the passivation of the lines. The results of this work are limited to concluding that (a) a combination of SiC inert particles and untreated lines does not work and that (b) treated lines under the absence SiC do work. Although it appears likely that line passivation is required, an experiment with untreated lines and without inert material should be conducted to provide a final conclusive validation.

The effect of steam on the distribution of phosphorus in the μ-fixed-bed remains unclear. Although initial findings hint that phosphorus dosing should occur in conjunction with the introduction of steam, further experiments including steam need to be carried out to prove or refute this hypothesis. Further work should now be devoted toward conducting kinetic experiments and deriving a suitable model, free of transport limitations, for the phosphorus dynamics of the VPO catalyst. A combination of transport limitation free reaction kinetics and phosphorus dynamics would allow for the independent description of the molecular scale processes in selective *n*-butane oxidation and would pose a major step on the path toward improved modeling of industrial MA reactors.

ASSOCIATED CONTENT

Supporting Information

The Supporting Information is available free of charge at https://pubs.acs.org/doi/10.1021/acs.iecr.3c02604.

Detailed description of the experimental setup and preparation of the μ-catalyst and passivation procedure, including photographs and schematics (PDF)

https://doi.org/10.1021/acs.iecr.3c02604
Ind. Eng. Chem. Res. XXXX, XXX, XXX−XXX

AUTHOR INFORMATION

Corresponding Author

Scott D. Anderson − *Institute of Chemical and Electrochemical Process Engineering, Clausthal University of Technology, Clausthal-Zellerfeld 38678, Germany;* orcid.org/0000-0002-9805-7755; Phone: +49 5323 722181; Email: anderson@icvt.tu-clausthal.de; Fax: +49 5323 722181

Authors

Martin Kutscherauer − *Clariant AG, Heufeld 83052, Germany; Institute of Chemical and Electrochemical Process Engineering, Clausthal University of Technology, Clausthal-Zellerfeld 38678, Germany*

Nicolas Nickel − *Institute of Chemical and Electrochemical Process Engineering, Clausthal University of Technology, Clausthal-Zellerfeld 38678, Germany*

Sebastian Böcklein − *Clariant AG, Heufeld 83052, Germany*

Gerhard Mestl − *Clariant AG, Heufeld 83052, Germany*

Gregor D. Wehinger − *Institute of Chemical and Electrochemical Process Engineering, Clausthal University of Technology, Clausthal-Zellerfeld 38678, Germany;* orcid.org/0000-0002-1774-3391

Thomas Turek − *Institute of Chemical and Electrochemical Process Engineering, Clausthal University of Technology, Clausthal-Zellerfeld 38678, Germany;* orcid.org/0000-0002-7415-1966

Complete contact information is available at: https://pubs.acs.org/10.1021/acs.iecr.3c02604

Notes

The authors declare no competing financial interest.

NOMENCLATURE

d diameter	m
GHSV gas hourly space velocity	$m^3\ m^{-3}\ h^{-1}$
h Height	m
S selectivity	%
T temperature	K or °C
T_{SBT} salt bath temperature	°C
x mole Fraction	-
X conversion	%
Δ absolute difference	various
ϵ error	-
η_{cat} catalyst effectiveness factor	%
1D	one dimensional
2D	two dimensional
DOS	days on stream
EDX	energy-dispersive X-ray spectroscopy
MA	maleic anhydride
SiC	silicon carbide
TMP	trimethyl phosphate
TOS	time on stream
VPO	vanadium phosphorus oxide
VPP	vanadyl-pyrophosphate
cat	catalyst
p	particle

REFERENCES

(1) Guan, M.; Kishi, A.; Linak, E.; Buchholz, U. *Chemical Economics Handbook*; IHS Markit, 2018.

(2) Freerks, M.; Suda, M. Production of maleic anhydride by catalytic oxidation of saturated aliphatic hydrocarbons. U.S. Patent 3,832,359 A, 1974.

(3) Freerks, M.; Suda, M. Catalyst for n-butane oxidation to maleic anhydride. U.S. Patent 3,864,280 A, 1975.

(4) Felthouse, T. R.; Burnett, J. C.; Horrell, B.; Mummey, M. J.; Kuo, Y.-J. *Kirk-Othmer Encyclopedia of Chemical Technology*; John Wiley & Sons, Ltd, 2001; Vol. *15*, pp 1−49.

(5) Volta, J.-C. Vanadium phosphorus oxides, a reference catalyst for mild oxidation of light alkanes: a review. *C. R. Acad. Sci.* **2000**, *3*, 717−723.

(6) Müller, M.; Kutscherauer, M.; Böcklein, S.; Wehinger, G.; Turek, T.; Mestl, G. Modeling the selective oxidation of n-butane to maleic anhydride: From active site to industrial reactor. *Catal. Today* **2022**, *387*, 82−106.

(7) Lesser, D.; Mestl, G.; Turek, T. Transient behavior of vanadyl pyrophosphate catalysts during the partial oxidation of n-butane in industrial-sized, fixed bed reactors. *Appl. Catal., A* **2016**, *510*, 1−10.

(8) Trifirò, F.; Grasselli, R. K. How the yield of maleic anhydride in n-butane oxidation, using VPO catalysts, was improved over the years. *Top. Catal.* **2014**, *57*, 1188−1195.

(9) Ballarini, N.; Cavani, F.; Cortelli, C.; Ligi, S.; Pierelli, F.; Trifiro, F.; Fumagalli, C.; Mazzoni, G.; Monti, T. VPO catalyst for n-butane oxidation to maleic anhydride: A goal achieved, or a still open challenge? *Top. Catal.* **2006**, *38*, 147−156.

(10) Wellauer, T. P.; Cresswell, D.; Newson, E. Optimal policies in maleic anhydride production through detailed reactor modelling. *Chem. Eng. Sci.* **1986**, *41*, 765−772.

(11) Müller, M.; Kutscherauer, M.; Böcklein, S.; Mestl, G.; Turek, T. Improved Kinetics of n-Butane Oxidation to Maleic Anhydride: The Role of Byproducts. *Ind. Eng. Chem. Res.* **2021**, *60*, 218−229.

(12) Ebner, J. R. Method for Improving the Performance of VPO Catalysts. U.S. Patent 5,185,455 A, 1993.

(13) Diedenhoven, J.; Reitzmann, A.; Mestl, G.; Turek, T. A Model for the Phosphorus Dynamics of VPO Catalysts during the Selective Oxidation of n-Butane to Maleic Anhydride in a Tubular Reactor. *Chem. Ing. Technol.* **2012**, *84*, 517−523.

(14) Edwards, R. Process for Improving Phosphorus-Vanadium Oxide and Phosphorus-Vanadium-Co-Metal Oxide Catalysts. U.S. Patent 4,701,433 A, 1987.

(15) Edwards, R. Process for Regenerating and Stabilizing Phosphorus-Vanadium-Oxygen Complex Catalysts. U.S. Patent 4,861,738 A, 1989.

(16) Taheri, H. Continuous Process for the Production of Maleic Anhydride from a C4-Hydrocarbon Feedstock. U.S. Patent 5,117,007 A, 1992.

(17) EPA. *Overview of Greenhouse Gases*, online, 2023, https://www.epa.gov/ghgemissions/overview-greenhouse-gasewebs, (visited on 22.08.2023).

(18) National Research Council. *Carbon Management: Implications for R&D in the Chemical Sciences and Technology*, 2001.

(19) Lesser, D.; Mestl, G.; Turek, T. Modeling the dynamic behavior of industrial fixed bed reactors for the manufacture of maleic anhydride. *Chem. Eng. Sci.* **2017**, *172*, 559−570.

(20) Brandstädter, W. M.; Kraushaar-Czarnetzki, B. Maleic anhydride from mixtures of n-butenes and n-butane: effective reaction kinetics. *Ind. Eng. Chem. Res.* **2005**, *44*, 5550−5559.

(21) Gascón, J.; Valenciano, R.; Téllez, C.; Herguido, J.; Menéndez, M. A generalized kinetic model for the partial oxidation of n-butane to maleic anhydride under aerobic and anaerobic conditions. *Chem. Eng. Sci.* **2006**, *61*, 6385−6394.

(22) Lorences, M. J.; Patience, G. S.; Diez, F. V.; Coca, J. Butane oxidation to maleic anhydride: kinetic modeling and byproducts. *Ind. Eng. Chem. Res.* **2003**, *42*, 6730−6742.

(23) Uihlein, K. Butanoxidation an VPO-Wirbelschichtkatalysatoren. Ph.D. Thesis, Technische Hochschule Karlsruhe, 1993.

(24) Lerou, J.; Mills, P. *Precision Process Technology: Perspectives for Pollution Prevention*; Springer, 1993; pp 175−195.

https://doi.org/10.1021/acs.iecr.3c02604
Ind. Eng. Chem. Res. XXXX, XXX, XXX−XXX

(25) Centi, G.; Fornasari, G.; Trifiro, F. n-Butane oxidation to maleic anhydride on vanadium-phosphorus oxides: kinetic analysis with a tubular flow stacked-pellet reactor. *Ind. Eng. Chem. Prod. Res. Dev.* **1985**, *24*, 32−37.
(26) Buchanan, J.; Sundaresan, S. Kinetics and redox properties of vanadium phosphate catalysts for butane oxidation. *Appl. Catal.* **1986**, *26*, 211−226.
(27) Müller, M.; Junge, K.; Mestl, G.; Turek, T. Millistructured reactor as tool for investigating the kinetics of maleic anhydride synthesis. *Chem. Ing. Technol.* **2020**, *92*, 575−581.
(28) Müller, M.; Kutscherauer, M.; Böcklein, S.; Mestl, G.; Turek, T. On the importance of by-products in the kinetics of n-butane oxidation to maleic anhydride. *Chem. Eng. J.* **2020**, *401*, 126016.
(29) Hofmann, S.; Turek, T. Process Intensification of n-Butane Oxidation to Maleic Anhydride in a Millistructured Reactor. *Chem. Eng. Technol.* **2017**, *40*, 2008−2015.
(30) Mestl, G.; Lesser, D.; Turek, T. Optimum performance of vanadyl pyrophosphate catalysts. *Top. Catal.* **2016**, *59*, 1533−1544.
(31) Arnold, E. W.; Sundaresan, S. Effect of water vapor on the activity and selectivity characteristics of a vanadium phosphate catalyst towards butane oxidation. *Appl. Catal.* **1988**, *41*, 225−239.
(32) Zanthoff, H.; Sananes-Schultz, M.; Buchholz, S.; Rodemerck, U.; Kubias, B.; Baerns, M. On the active role of water during partial oxidation of n-butane to maleic anhydride over (VO) 2P2O7 catalysts. *Appl. Catal., A* **1998**, *172*, 49−58.
(33) Kubias, B.; Richter, F.; Papp, H.; Krepel, A.; Kretschmer, A. *Third World Congress on Oxidation Catalysis*; Elsevier, 1997; p 461.
(34) Patience, G. S.; Bockrath, R. E.; Sullivan, J. D.; Horowitz, H. S. Pressure calcination of VPO catalyst. *Ind. Eng. Chem. Res.* **2007**, *46*, 4374−4381.
(35) Puttock, S. J.; Rochester, C. H. Infrared study of water and pyridine adsorption on the surface of anhydrous vanadyl pyrophosphate. *J. Chem. Soc., Faraday Trans.* **1986**, *82*, 2773−2779.
(36) Ihli, J.; Bloch, L.; Boecklein, S.; Rzepka, P.; Burghammer, M.; Cesar da Silva, J.; Mestl, G.; Anton van Bokhoven, J. Evolution of Heterogeneity in Industrial Selective Oxidation Catalyst Pellets. *ACS Catal.* **2021**, *11*, 8274−8283.
(37) Wilkinson, S.; Simmons, M.; Stitt, E.; Baucherel, X.; Watson, M. A novel approach to understanding and modelling performance evolution of catalysts during their initial operation under reaction conditions−Case study of vanadium phosphorus oxides for n-butane selective oxidation. *J. Catal.* **2013**, *299*, 249−260.
(38) Granados, M. L.; Fierro, J. G.; Cavani, F.; Colombo, A.; Giuntoli, F.; Trifirò, F. Study by XPS and TPD of the interaction of n-pentane and n-butane with the surface ofnon-equilibrated'andequilibrated'V−P−O catalysts. *Catal. Today* **1998**, *40*, 251−261.
(39) Centi, G.; Trifiro, F.; Ebner, J. R.; Franchetti, V. M. Mechanistic aspects of maleic anhydride synthesis from C4 hydrocarbons over phosphorus vanadium oxide. *Chem. Rev.* **1988**, *88*, 55−80.
(40) Gai, P. L.; Kourtakis, K.; Coulson, D. R.; Sonnichsen, G. C. HREM microstructural studies on the effect of steam exposure and cation promoters on vanadium phosphorus oxides: New correlations with n-butane oxidation reaction chemistry. *J. Phys. Chem. B* **1997**, *101*, 9916−9925.
(41) Bej, S. K.; Rao, M. S. Selective oxidation of n-butane to maleic anhydride. 3. Modeling studies. *Ind. Eng. Chem. Res.* **1991**, *30*, 1829−1832.
(42) Click, G. T.; Barone, B. J. Steam regeneration of phosphorus treated vanadium-phosphorus-oxygen catalysts. U.S. Patent 4,515,899 A, 1985.
(43) Haddad, M. S.; Goeden, G. V. Novel phosphorus addition process for improvement of catalysts suitable for maleic anhydride production. U.S. Patent 7,629,286 B2, 2009.
(44) Dong, Y.; Geske, M.; Korup, O.; Ellenfeld, N.; Rosowski, F.; Dobner, C.; Horn, R. What happens in a catalytic fixed-bed reactor for n-butane oxidation to maleic anhydride? Insights from spatial profile measurements and particle resolved CFD simulations. *Chem. Eng. J.* **2018**, *350*, 799−811.
(45) IFA. GESTIS-Stoffdatenbank: Trimethylphosphat. 2023, https://gestis.dguv.de/data?name=04153web0, (accessed 09 01, 2023).
(46) Kihira, H.; Ito, S.; Murata, T. The behavior of phosphorous during passivation of weathering steel by protective patina formation. *Corros. Sci.* **1990**, *31*, 383−388.
(47) Flis, J.; Mańkowski, J.; Zakroczymski, T.; Bell, T. The formation of phosphate coatings on nitrided stainless steel. *Corros. Sci.* **2001**, *43*, 1711−1725.
(48) Lakatos-Varsányi, M.; Falkenberg, F.; Olefjord, I. The influence of phosphate on repassivation of 304 stainless steel in neutral chloride solution. *Electrochim. Acta* **1998**, *43*, 187−197.
(49) Cavani, F.; Luciani, S.; Esposti, E. D.; Cortelli, C.; Leanza, R. Surface dynamics of a vanadyl pyrophosphate catalyst for n-butane oxidation to maleic anhydride: an in situ raman and reactivity study of the effect of the P/V atomic ratio. *Chem.—Eur. J.* **2010**, *16*, 1646−1655.

https://doi.org/10.1021/acs.iecr.3c02604
Ind. Eng. Chem. Res. XXXX, XXX, XXX−XXX